MECSOL 2019 - Proceedings of the 7th International Symposium on Solid Mechanics,
V. Tita, A. Ferreira, M.L. Ribeiro, A. Vieira and A.T. Beck (Editors), ABCM, Sao Carlos, SP, Brazil, April 15th to 17th, 2019

Exploring the performance advantage of an additively manufactured viscoelastic metamaterial for use as a helmet liner

Rhosslyn Adams [1], Shwe Soe [1], Roy Burek [1, 2], Michael Robinson [1], Ben Hanna [1], Peter Theobald[1]

[1] Cardiff School of Engineering, Cardiff University, The Parade, Cardiff, CF24 3AA, UK.

[2] Charles Owen & Co (Bow) Ltd, Croesfoel Industrial Park, Wrexham, LL14 4BJ, UK.

Existing head impact protection solutions exhibit a very narrow performance window, offering effective protection only at relatively high impact energies. This study explores whether additive manufacturing can be used to design a new family of materials and, thus, achieve a more effective solution for a range of impact energies. The 'Miura-ori' stacked folding origami pattern has inspired a series of metamaterial structures that have been highlighted for exemplar performance against contemporary energy-absorbing systems. This work develops on our previous success by leveraging the established impact attenuating ability of viscoelastic rubber-like materials, achieved through Inkjet additive manufacturing. To this end, as-printed material properties were compared to supplier data for 3 co-polymers, whilst Miura-Ori structures were quasistatically compressed and impacted, at increasing velocities. Comparison was drawn against the current state of the art, Vinyl Nitrile, as well as our previous design iteration manufactured using Selective Laser Sintering. Results indicated that a viscoelastic Miura-ori structure achieved improved absorption of peak linear acceleration, versus Vinyl Nitrile.

Keywords: Viscoelastic, Additive Manufacturing, Impact, Head protection, Helmet

INTRODUCTION

Activities that present a severe head injury risk typically utilise foam-lined helmets to provide enhanced protection. Foams deliver a highly effective mechanism of energy absorption and are light-weight, meaning that they are ideal for personal protection equipment applications. Energy absorption, for cellular materials, is performed by deformation of the cell walls, achieving highly effective absorption from linear / translational (i.e. 'vertical') impacts. Sports-related helmets commonly employ expanded polystyrene (EPS) and vinyl nitrile (VN) foams for single- and multi-impact environments respectively; however, both are long-established materials that have recognized limitations and there is scope for them to be outperformed by novel solutions. This study focuses on identifying novel helmet solutions that offer effective energy absorption across a wider range of impact energies than the identified existing materials. Success would achieve greater energy absorption and so enhanced head protection, during impact scenarios.

Additive manufacturing (AM) has supported a surge in interest in impact mitigating cellular materials, with most current work focusing on prismatic (honeycomb), and strut-based periodic lattice structures. The layer-by-layer fabrication of AM offers unprecedented access to novel geometries and material-geometry combinations, providing opportunity to manufacture structures with superior weight/performance ratios, versus contemporary materials (Brennan-Craddock, Brackett, Wildman, & Hague, 2012; Smith, Guan, & Cantwell, 2013). Whilst investigation continues to explore the mechanical potential of these types of traditional cellular structures (Soe, Martin, Jones, Robinson, & Theobald, 2015; Soe, Ryan, McShane, & Theobald, 2015), their potential for achieving best-in-class performance in demanding applications, such as those with challenging material thickness constraints and complex load cases, remains to be proven. In addition to the added complexity offered by AM, access is increasing to exotic material families, with the mechanical properties and processing parameters of AM elastomers being reported in literature (Soe, Martindale, Constantinou, & Robinson, 2014; Verbelen et al., 2017).

Viscoelastic elastomers are known to act as excellent shock absorbers. They enhance damping by reducing the associated impulse of an impact, affording a lower rebound compared to conventional engineering materials. Furthermore, due to their rate-dependent nature, application of viscoelastic materials would prove an exciting opportunity to enhance the narrow performance window of current helmet liner alternatives. Viscoelastic materials have been successfully exploited in sporting equipment with relative insensitivity to weight, such as shoes and protective pads, reducing the force transmitted and thus lowering injury risk (O'Leary, Vorpahl, & Heiderscheit, 2008). Little

success has been realized, however, in applying this benefit to the head protection sector, where designs are constrained to a 'wearable' weight (Roseveare, Plant, & Ghajari, 2016).

This paper builds upon our previous work that demonstrated the superior performance of an elastomeric, origami-inspired structure (hereafter termed the 'Miura-ori' (MO)), versus the traditional VN helmet liner material (Robinson, M, Soe, S. P., G, McShane, Theobald, 2017). It now describes the use and potential advantage of a novel, viscoelastic AM material to further enhance performance of the MO structure with respect to previous design iterations.

MATERIALS AND METHODS

A literature review of additive manufacturing methods identified the Inkjet process as an appropriate means to achieve customizable viscoelasticity, i.e. achieving variable storage and loss moduli, which are important in material selection for dynamic loading where the storage moduli is associated with the elastic energy returned and loss moduli the viscous energy dissipated (MacCurdy, Lipton, Li, & Rus, 2016). The Inkjet process builds up layers of photopolymers that are cured using ultraviolet light (similarly to most Stereolithographic processes); however, the deposited material is derived from two co-components that are simultaneously mixed, to varying extents, to achieve a broad range of mechanical properties. The Objet Conex 500 printer (Stratasys, Minnesota, US), an AM machine which is enabled by the Inkjet, utilizes different ratios of distinct base materials: "TangoBlack", an elastomeric material and "VeroWhite", a rigid polymer. Mixing to varying extents produces new materials with overall homogenous bulk properties.

The mechanical properties, including static and dynamic, as well as the influence of build orientation of Inkjet fabricated parts has been documented within the literature. Of note, the frequency and temperature dependent viscoelastic properties for vibration dampening applications is reported, illustrating a significant frequency dependency (Reichl & Inman, 2018) - equivalent to strain-rate sensitivity. Although Inkjet is typically considered a process for 'prototyping' products which use rubber-like materials, the ability to additively manufacture structures with material properties that exhibit strain rate sensitivity is uncommon. Hence, it may prove advantageous to further explore impact mitigation using this manufacturing process.

For the Objet Connex 500 printer, ten "off the shelf" optimized material solutions are available as defined by their shore A hardness values. Selecting an appropriate material solution proved challenging given the lack of any in-house reference data. Three co-polymer blends were selected based on the shore A hardness of our existing solution, which coincided with the upper bound of the available Inkjet materials. These were material solutions with Shore Hardness 95, 85 and 60 A – hereafter referred to as A, B and C respectively.

The three material solutions were used to manufacture an MO structure, of identical geometric dimensions to that which was previously investigated, with a surface-area equivalent to a standard NFL helmet pad (Figure 1), and a slab sample of nominal dimensions 60 x 25 x 5 mm. The MO structure was tested under quasistatic compression to better understand the interplay between the base material and geometric structure, whilst impact loading was performed to determine the efficacy of each structure in a load regime comparable to the end application. Slab samples were used for Shore hardness testing to cross-validate the manufacturer provided information (Table 1). Comparative data was generated for a vinyl nitrile (VN) pad, exhumed from a commercially available American football helmet (Rawlings, Missouri, US), and our previous design iteration fabricated using selective laser sintering (SLS) (Lehmann & Voss, Hamburg, Germany), hereafter referred to as SLS-MO, to produce a baseline for impact testing.

Table 1 – Manufacturer provided material properties of Objet Connex digital materials printed using base materials VeroWhitePlus and TangoPlus.

Sample	Material	Shore A value	Elongation at break (%)	Tensile strength (MPa)
A	DM 9795	90 – 95	25 – 35	15 – 25
B	DM 9785	80 – 85	50 – 60	4 – 8
C	DM 9760	57 – 63	80 – 100	2 – 4

Shore A hardness testing was carried out using a Durometer (HBA 100-0; Sauter, GmbH, Balingen, Germany) on the slab samples. Data was measured in accordance with ASTM D 2240-86 and ISO 868, at regular intervals along the specimen length. A minimum dwell time of 1s was adopted to minimize viscoelastic creep effects and tests were carried out at ambient temperature.

Quasistatic compression testing was performed using a universal mechanical tester (Z50, Zwick Roell Group, Ulm, Germany) between two metallic platens treated with lubricant to reduce the evolution of friction, at a crosshead

displacement rate of 10 mm/min. Load and displacement was measured with a 50 kN load cell and crosshead travel respectively.

Impact testing was performed using a drop-weight impact tower (Dynatup 8250, Instron, Massachusetts, US). Data was measured via a 50 kN load cell located in-line with the centre impacting platen and was recorded at 50 kHz via a data acquisition system. Each specimen was taped in place to the centre of a rigid anvil and a 5kg impacting platen was rail-guided, under free-fall, onto the sample. Each sample was subjected to 4 impacts through 2 – 5 m/s at 1 m/s interval, representative of in-situ loading conditions. Ample relaxation time was provided between impacts to mitigate stress softening.

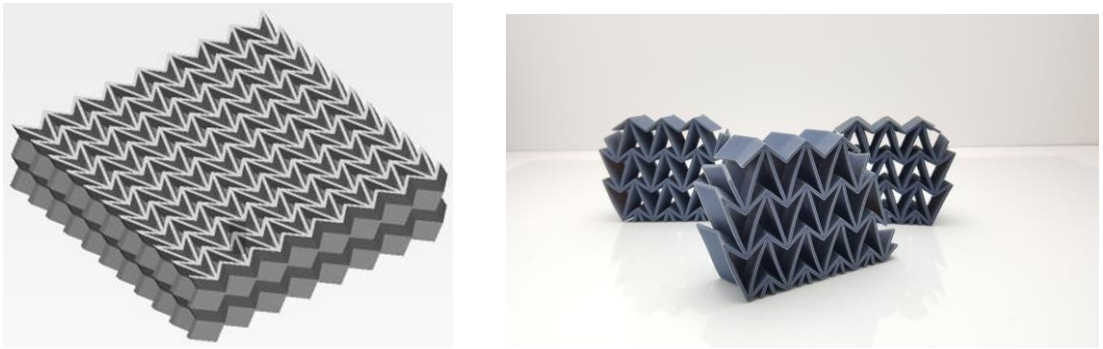

Figure 1 – (a) CAD representation of the MO design, (b) Objet manufactured parts, sized to VN sample dimensions.

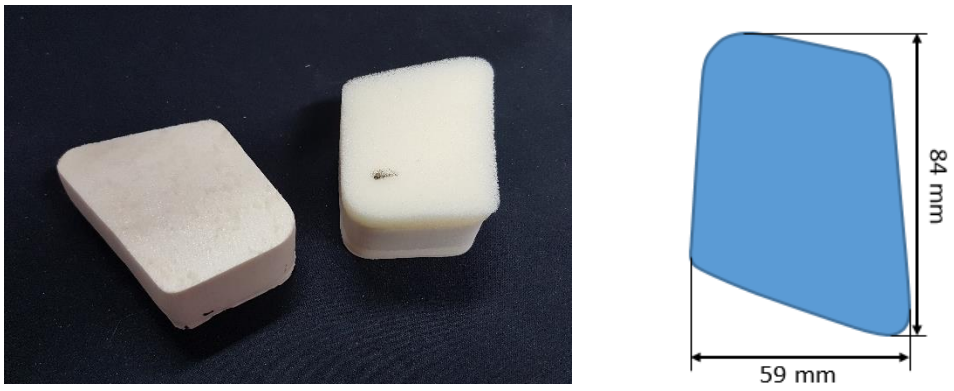

Figure 2 – (a) The two VN parts removed from the American football helmet, one shown (L) following removal of the comfort liner, (b) dimensions of the trimmed foam samples.

RESULTS AND DISCUSSION

Shore hardness:

The hardness data for materials A, B and C is presented in Table 2. Specimens A, B and C were calculated to have an average value (n = 5) of 93, 87 and 65 Shore A respectively. Specimen A was found to lie within the range specified by the manufacturer; however, specimens B and C fell outside. Standard deviation for the measured values was calculated as 2.2, 2.9 and 3.5. Significant variation was observed across the specimen length, indicating a non-homogenous or graded overall material was achieved, either due to inadequate optimization of the process setting or due to limitations in achieving a homogenously mixed distributed material. It would seem, therefore, that while this process provides opportunity for customizable material behavior per part, it currently lacks the control to achieve a consistent quality within each build, limiting its application within mass manufacturing where such traits are critical.

Table 2 – Manufacturer provided material properties of Object Connex digital materials printed using base materials VeroWhitePlus and TangoPlus.

Specimen	Material	Shore A hardness values				
		Expected	Avg.	Max	Min	SD
A	DM 9795	95-90	93	95	90	2.2
B	DM 9785	85-80	87	90	83	2.9
C	DM 9760	63-57	65	70	61	3.5

Quasistatic compression:

Load-displacement curves for quasistatic compression of the three Inkjet MO samples are shown in Figure 4 (a). It is important to note that due to the quasistatic loading regime, the effect of strain rate sensitivity is mitigated and therefore this behavior is representative of the static hyperelastic material behaviour, in conjunction with the MO structure kinematics. The samples exhibit characteristic behavior of cellular solids under compression, i.e. a sharp rise in initial stiffness, before reaching a critical load that achieves deformation identified by an established plateau region. Further deformation achieves a state of densification where the load sharply increases again. Very little energy is absorbed in the initial region; however, the long plateau region, which is representative of cell walls buckling and collapsing, allows for large energy-absorption at a constant load. Whilst the previous statements describes the behavior of an ideal cellular solid (i.e. closed cell foam), the MO is considered an auxetic material; that is, it is a material which demonstrates a negative Poisson's ratio under deformation (Schenk, Guest, & McShane, 2014). Auxetic structures similarly display an initial stiffness, followed by a plateau region; however, this region exhibits a less stable peak value and instead presents stiffening until densification, as more material is drawn towards the centre (Allen et al., 2017).

Each specimen achieves a different peak plateau load, which can be considered a function of the base material as each comprise the same geometrical structure. The initial stiffness of A and B are similar and probably have a higher relative base material modulus than C, as inferred from manufacturer material information. These structures, therefore, resist deformation, exhibiting greater buckling before the peak plateau load (a function of both the material and the geometric structure). The compliancy of C does not provide the same resistance to deformation and therefore the structural response is less dominant or significant.

As each specimen had the same geometric structure, it was expected that identical densification strains would be achieved; however, contrary evidence is presented in the load-displacement curve. The kinematics of the MO structures are based on the collapse of a rigid distinctive folding mechanism. With the application of elastomeric materials, which in this case varied from specimen to specimen, it is postulated that the kinematic response is affected. Rather than buckling and folding along the contours of the MO (as it is designed to), buckling and bending occurred across the sheets as well as warping at the top of the chevrons between neighbouring unit cells. A rigid material would have a more established and defined section to its force-displacement behaviour. There seems significant interplay between the base material and the overall MO kinematic structural response. Materials which exhibit high viscoelasticity are typically more compliant and, thus, may not be well suited to this structure, due to the failure modes requiring exact folding along its contours to achieve a controlled collapse and stable peak load. Since the effects of strain-rate sensitivity have been isolated it is expected that under dynamic loading (i.e. impact) with inertial effects considered, these structures will show a different behavior.

Dynamic impact:

The results of the impact testing identified that samples A and B were not appropriate for further consideration, achieving a peak g which far exceeded that of VN or the SLS-MO. The results of A and B are attributed to inappropriate selection of the base material. At the impact velocities tested the structure did not initiate the folding mechanism of the MO structure, thus was not able to achieve controlled deformation and so resulted in a bulk transfer of kinetic energy and a large peak g.

Sample C showed promising results, with the relative performance in peak linear acceleration absorption plotted against reference data (Figure 4 (b)). Interesting dynamic behaviour was demonstrated across a range of impact velocities, particularly at higher velocities. Here, the material produced lower impact accelerations than either the VN or SLS-MO data. Acceleration values at lower velocity was comparable to the other materials. Considering the gradient of sample C in Figure 4 (b), a linear stepwise increase in peak g is observed, demonstrating a strain-rate sensitivity that is thought to be a result of enhanced viscoelastic material behaviour. Upon densification of sample C through the MO folding mechanism, it is expected that no more work can be done; however, it is further hypothesized that as the

material is compressed the bulk mass of viscoelastic material dissipates additional energy through viscous dampening. This hypothesis requires additional substantiation and will be developed in supplementary work.

When considering the VN and SLS-MO baseline data, at low impact velocity they operate effectively achieving low values for peak g, although are unable to perform at high impact velocity. This is due to the occurrence of densification, which causes a bulk transfer of unmitigated kinetic energy. Again considering Figure 4 (b), the VN and SLS-MO curves show relatively linear stepwise increases in peak g for the low velocity impacts; however, at higher velocity impacts, sharp up-turns in the curves are observed, identifying loading regimes for which they are not optimized and so causing a high peak g. Arguably to achieve better performance in this regime, a stiffer material or different geometric structure could be selected; however, this would then prove unfavorable at lower impact velocities. This warrants further investigation of the associated advantages of utilizing a viscoelastic material.

It is important to note that the longevity of Inkjet printed parts is a severe shortcoming compared to other AM fabricated parts such as Fused filament Fabrication and Selective Laser Sintering. After repeat testing, degradation was observed at the top of chevrons and across planar faces of the MO. This is thought to be attributed to a low tensile strength and elongation at break, which increased its propensity to tear and fracture. The magnitude and occurrence of this degradation was less significant when comparing A to B and B to C.

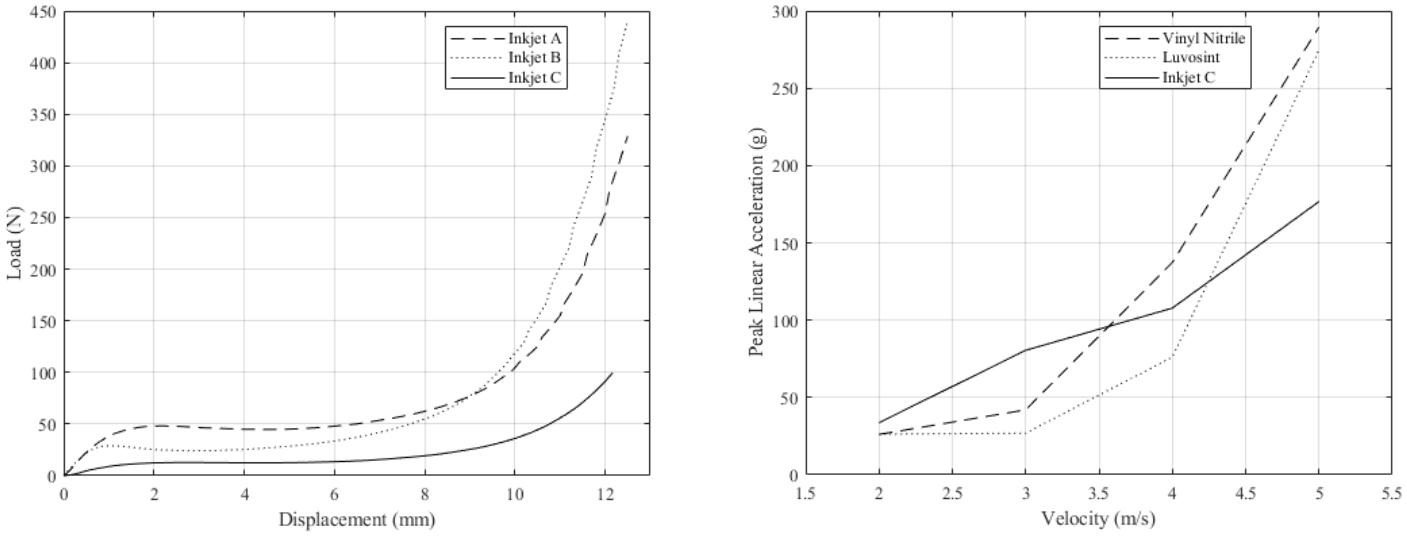

Figure 4 – (a) Load-displacement curve for Inkjet A (dash), Inkjet B (dot) and Inkjet C (solid), (b) Relative performance in peak linear acceleration for Vinyl Nitrile (dash), Luvosint (dot) and Inkjet C (solid).

CONCLUSIONS

The application of an additively manufactured viscoelastic material to the MO structure has demonstrated potential to enhance energy absorption. Further investigation is currently being conducted to understand the precise material behaviour, such that with an improved understanding of the inter-play between the geometric structure and material, we can establish a more effective energy absorbing system. This work provides the first indication that AM may provide a successful route to incorporating viscoelastic materials into head protection systems.

ACKNOWLEDGMENTS

The authors acknowledge the financial support of Charles Owen & Co (Bow) Ltd.

REFERENCES

Allen, T., Duncan, O., Foster, L., Senior, T., Zampieri, D., Edeh, V., & Alderson, A. (2017). Auxetic Foam for Snow-

Sport Safety Devices. In *Internation Society for Skiing Safety*. https://doi.org/10.1007/978-3-319-52755-0

Brennan-Craddock, J., Brackett, D., Wildman, R., & Hague, R. (2012). The design of impact absorbing structures for additive manufacture. *Journal of Physics: Conference Series*, *382*(1), 012042. https://doi.org/10.1088/1742-6596/382/1/012042

MacCurdy, R., Lipton, J., Li, S., & Rus, D. (2016). Printable programmable viscoelastic materials for robots. In *2016 IEEE/RSJ International Conference on Intelligent Robots and Systems (IROS)* (pp. 2628–2635). IEEE. https://doi.org/10.1109/IROS.2016.7759409

O'Leary, K., Vorpahl, K. A., & Heiderscheit, B. (2008). Effect of Cushioned Insoles on Impact Forces During Running. *Journal of the American Podiatric Medical Association*, *98*(1), 36–41. https://doi.org/10.7547/0980036

Reichl, K. K., & Inman, D. J. (2018). Dynamic Mechanical and Thermal Analyses of Objet Connex 3D Printed Materials. *Experimental Techniques*, *42*(1), 19–25. https://doi.org/10.1007/s40799-017-0223-0

Robinson, M, Soe, S. P., G, McShane, Theobald, P. (2017). Developing Elastomer Cellular Structures for Multiple Head Impacts. *IRCOBI Conference 2017*, 182–189.

Roseveare, A., Plant, D., & Ghajari, M. (2016). A New Helmet-liner Design for Improved Survivability. *IRCOBI Conference 2016*, 424–425.

Schenk, M., Guest, S. D., & McShane, G. J. (2014). Novel stacked folded cores for blast-resistant sandwich beams. *International Journal of Solids and Structures*, *51*(25–26), 4196–4214. https://doi.org/10.1016/j.ijsolstr.2014.07.027

Smith, M., Guan, Z., & Cantwell, W. J. (2013). Finite element modelling of the compressive response of lattice structures manufactured using the selective laser melting technique. *International Journal of Mechanical Sciences*, *67*, 28–41. https://doi.org/10.1016/J.IJMECSCI.2012.12.004

Soe, S. P., Martin, P., Jones, M., Robinson, M., & Theobald, P. (2015). Feasibility of optimising bicycle helmet design safety through the use of additive manufactured TPE cellular structures. *The International Journal of Advanced Manufacturing Technology*, *79*(9–12), 1975–1982. https://doi.org/10.1007/s00170-015-6972-y

Soe, S. P., Martindale, N., Constantinou, C., & Robinson, M. (2014). Mechanical characterisation of Duraform® Flex for FEA hyperelastic material modelling. *Polymer Testing*, *34*, 103–112. https://doi.org/10.1016/j.polymertesting.2014.01.004

Soe, S. P., Ryan, M., McShane, G., & Theobald, P. (2015). Energy absorption characteristics of additively manufactured TPE cellular structures. Retrieved from http://orca.cf.ac.uk/73193/

Verbelen, L., Dadbakhsh, S., Van den Eynde, M., Strobbe, D., Kruth, J.-P., Goderis, B., & Van Puyvelde, P. (2017). Analysis of the material properties involved in laser sintering of thermoplastic polyurethane. *Additive Manufacturing*, *15*, 12–19. https://doi.org/10.1016/J.ADDMA.2017.03.001

RESPONSIBILITY NOTICE

The authors are the only responsible for the printed material included in this paper.